ELSEVIER

Journal of Fluids and Structures 23 (2007) 633–647

JOURNAL OF FLUIDS AND STRUCTURES

www.elsevier.com/locate/jfs

Wave scattering by flexible porous vertical membrane barrier in a two-layer fluid

P. Suresh Kumar, S.R. Manam, T. Sahoo*

Department of Ocean Engineering and Naval Architecture, Indian Institute of Technology, Kharagpur 721302, India

Received 4 February 2004; accepted 30 October 2006
Available online 22 December 2006

Abstract

The scattering of water waves by a flexible porous membrane barrier in a two-layer fluid having a free surface is analysed in two dimensions. The membrane barrier is extended over the entire water depth in a two-layer fluid, each fluid being of finite depth. In the present analysis, linear wave theory and small amplitude membrane response are assumed. The porous membrane barrier is tensioned and pinned at both the free surface and the seabed. The associated mixed boundary value problem is reduced to a linear system of equations by utilizing a general orthogonality relation along with least-squares approximation method. Because of the flow discontinuity at the interface, the eigenfunctions involved have a discontinuity at the interface and the orthogonality relation used is a generalization of the classical one corresponding to a single-layer fluid. The reflection and transmission coefficients for the surface and internal modes, the free surface and interface elevations and the nondimensional membrane deflection are computed for various physical parameters like the nondimensional tension parameter, porous-effect parameter, fluid density ratio, ratio of water depths of the two fluids to analyse the efficiency of a porous membrane as a wave barrier in the two-layer fluid.

Keywords: Flexible; Porous; Membrane; Barrier; Surface wave; Internal wave

1. Introduction

In the recent past, flexible breakwaters with high wave dissipating ability have been considered as better than fixed rigid breakwaters for providing protection from wave attack in semi-protected regions or in areas where protection is required only on a temporary basis. For temporary wave barriers, the amplitude of the wave force is one of the primary concerns, as these structures do not have proper foundations or strong supports. Therefore, a characteristic of flexibility is usually included in these temporary barriers in order to minimize the wave forces on them. Leach et al. (1985) investigated the wave diffraction by a floating rigid breakwater and showed better efficiency of such breakwaters compared to fixed rigid breakwaters. Sollitt et al. (1986) examined a system composed of two buoyant flaps clamped at the sea bottom and coupled with weighted mooring lines. Lee and Chen (1990) and Williams et al. (1991) considered the case of a flexible breakwater consisting of a beam anchored to the seabed and tensioned by a buoy at the surface. Explicit solutions using Euler beam theory were obtained by Lee and Chen (1990), whilst Williams et al. (1991) used the boundary integral equation method to analyse the same problem. Results indicate that a relatively stiff structure was

*Corresponding author. Tel.: +91 3222 283792; fax: +91 3222 255303.
E-mail addresses: tsahoo@naval.iitkgp.ernet.in, tsahoo1967@yahoo.com (T. Sahoo).

0889-9746/$ - see front matter © 2006 Elsevier Ltd. All rights reserved.
doi:10.1016/j.jfluidstructs.2006.10.011

Nomenclature

d	thickness of the porous medium
f	resistance force coefficient
G	porous-effect parameter
g	acceleration due to gravity
H	total depth of entire fluid domain
h	depth of upper fluid
I_I, I_{II}	amplitude of incident wave in SM and IM
K	$=\omega^2/g$
k_0	incident wavenumber
Kr_I, Kr_{II}	reflection coefficient in surface mode (SM) and internal mode (IM)
Kt_I, Kt_{II}	transmission coefficient in SM and IM
m_s	membrane mass
m'	nondimensional membrane mass
p	wavenumber related to the frequency in the dispersion relation
P_s	differential pressure across the barrier
p_n	roots of dispersion relation
R_I, R_{II}	amplitude of reflected wave in SM and IM
s	two-layer fluid density ratio
s^*	inertial force coefficient
T	tension applied to the membrane
T_I, T_{II}	amplitude of transmitted wave in SM and IM
T'	nondimensional tension parameter
x, y	horizontal and vertical Cartesian coordinates
β	barrier frequency parameter
γ	porosity
ζ	barrier deflection (function of y and t)
$\eta_{\mathrm{fs}}, \eta_{\mathrm{int}}$	free surface and interface elevation
λ_I	wavelength of incident wave in SM
ξ	barrier deflection (function of y)
ρ_1, ρ_2	density of upper and lower fluid
ρ_s	membrane mass density
Φ	velocity potential (function of both *space* and *time*)
ϕ	spatial velocity potential
ω	wave frequency

needed to obtain a high wave reflection coefficient. Williams et al. (1991) analysed the wave diffraction due to a flexible breakwater consisting of a compliant, beam-like structure that was anchored to the sea bottom and kept under tension by a small buoyancy chamber at the top. Williams (1993) analysed the wave diffraction due to a pair of flexible breakwaters consisting of compliant, beam-like structures, also anchored to the sea bottom and kept under tension by a small buoyancy chamber at the top. Kim and Kee (1996) considered the case of a single flexible and inextensible membrane extending the entire water depth. Analytic and numerical solutions were developed. It was observed that membrane stiffness plays a significant role in barrier performance. Recently, flexible barriers consisting of vertical tensioned membranes spanning the entire water depth were reported. These include single membrane (Kim and Kee, 1996; Kee and Kim, 1997) and dual membrane arrangements (Cho et al., 1998; Lo, 1998). It was found that the wave transmission could be controlled primarily by the membrane tension in the case of a single structure, and in the case of a dual membrane arrangement, it was by the membrane spacing. Lo (2000) investigated the interaction of water waves with a vertical flexible membrane of a finite extent which is less than the water depth. The cases considered include that of a membrane descending from the water surface or ascending from the seabed, and that of an immersed membrane with gaps at both the top and the bottom. Lee and Lo (2002) studied the performance of surface-penetrating flexible membrane wave barriers of finite draft. They considered both single and dual membrane systems in their study.

Porous barriers are currently being suggested for wave dissipation, as reviewed by Chwang and Chan (1998). These kinds of porous barriers dissipate most of the incoming wave energy and reduce the wave forces on the barriers. Wang and Ren (1993) presented a theoretical study on the scattering of small amplitude waves by a flexible, porous and thin beam-like breakwater held fixed in the seabed. Using a least-squares method, Lee and Chwang (2000) studied the scattering and generation of water waves by vertical permeable barriers.

In all the aforementioned studies, free surface waves are considered for a fluid of constant density over the entire fluid domain. However, waves can also exist at the interface between two immiscible liquids of different densities. Such a sharp density gradient can, for example, be generated in the ocean by solar heating of the upper layer, or in an estuary or a fjord into which fresh (less saline) river water flows over oceanic water, which is more saline and consequently heavier. The situation can be idealized as a two-layer fluid by considering a lighter fluid of density ρ_1 lying over a heavier fluid of density ρ_2. The propagation of waves in a two-layer fluid with both a free surface and an interface (in the absence of any obstacles) was first investigated by Stokes (1847) and the classical problem of this type of two-layer fluid separated by a common interface with the upper fluid having a free surface is given in Lamb (1932, Art. 231) and Wehausen and Laitone (1960). In the case of a two-layer fluid having an interface and a free surface, two different propagating modes may be excited during the wave motion. The waves generated because of the presence of the free surface are referred to as surface modes (SM), whilst the waves generated because of the presence of the interface are

referred to as internal modes (IM) [see Milne-Thomson, 1996; Kundu and Cohen, 2002]. Linton and McIver (1995) developed a general theory for two-dimensional wave scattering by horizontal cylinders in an infinitely deep two-layer fluid, and calculated the amount of energy that was converted from one wavenumber to the other for the case of circular cylinders in either the upper or lower fluid layer. The motivation for their work came from a plan to build an underwater pipe bridge across one of the Norwegian fjords, bodies of water which typically consist of a layer of fresh water about 10 m thick on top of a very deep body of salt water. Work on three-dimensional scattering can be found in Yeung and Nguyen (1999) and Cadby and Linton (2000). In the former study, an integral equation technique was employed to solve radiation and diffraction problems for a rectangular barge in finite depth, whereas in the latter study, multi-pole expansions were used to solve problems involving submerged spheres in water of infinite depth. The symmetry relations for the added-mass and damping matrices and an analogue to the Haskind relations were given in Yeung and Nguyen (1999); a more complete derivation of reciprocity relations for three-dimensional scattering in two-layer fluids can be found in Cadby and Linton (2000). Other notable work on wave–structure interaction in two-layer fluids includes Zilman and Miloh (1995), Zilman et al. (1996) in which the effect of a shallow layer of fluid mud on the hydrodynamics of floating bodies was analysed. In Barthélemy et al. (2000), the scattering of surface waves by a step bottom in a two-layer fluid was considered. This problem is of particular interest to understand how tides are scattered at the continental shelf break. However, very little progress has been made on wave interaction with porous structures. Sherief et al. (2003) analysed the effect of gravity waves generated by a porous wave maker in a two-layer fluid with the upper fluid having a free surface. Recently, Manam and Sahoo (2005) tackled analytically the same problem of waves past rigid porous structures in two-layer fluid by making use of the generalized orthogonal relation. Also they obtained complete analytical solutions for the boundary value problems corresponding to the generation or scattering of axisymmetric waves by two impermeable and permeable coaxial cylinders.

In the present work, the performance of a flexible porous barrier in a two-layer fluid domain is investigated based on the linearized theory of water waves, with the upper fluid having a free surface. In the study, both layers of fluid are considered to be of finite depth and the flexible barrier is modelled as a thin and inextensible sheet of membrane subjected to uniform tension and homogeneous porosity. The membrane is assumed to be fixed end at both the free surface and the seabed. The reflection and energy dissipation characteristics of the system subjected to normal incident waves (one corresponding to a SM at the free surface and the other to an IM at the interface) are investigated. The boundary condition on the porous barrier has been developed by Yu and Chwang (1994), which is a generalization of the one developed by Chwang (1983) and the porous-effect parameter is a complex number, which includes both the inertia and resistance effects. The boundary value problem is solved by utilizing an orthogonality relation suitable for the two-layer fluid domain along with the least-squares approximation method. The behaviour of the energy transmission in both SM and IM, the variation of the nondimensional membrane modal amplitude and the pattern of free surface and interface elevation are investigated for various parameters of interest like nondimensional frequency parameter, water depth, fluid density ratio of the two-layer fluid, porous-effect parameter and tension applied to the membrane barrier.

2. Mathematical formulation

In the present work, the problem is analysed in a two-dimensional Cartesian coordinate system. The two fluids are assumed to be inviscid and incompressible and the wave motion is considered in the linearized theory of water waves neglecting the effect of surface tension. The fluids are separated by a common interface (undisturbed surface located at $y = h$), whereas the upper fluid has a free surface (undisturbed surface located at $y = 0$), and each fluid is of infinite horizontal extent ($-\infty < x < +\infty$); both the upper and lower fluids are of finite depth, $0 < y < h$ and $h < y < H$, respectively. Region 1 is defined as $-\infty < x < 0$, $0 < y < H$ and region 2 is defined as $0 < x < +\infty$, $0 < y < H$ (see Fig. 1). The porous membrane is located at $x = 0$, $0 < y < H$. The flow is assumed to be irrotational and simple harmonic in time with angular frequency ω. Therefore, the velocity potential Φ exists such that $\Phi_j(x, y, t) = \mathscr{R}e[\phi_j(x, y)\exp(-i\omega t)]$, where the spatial velocity potentials ϕ_j ($j = 1, 2$) satisfy the Laplace equation

$$\nabla^2\phi_j = 0 \quad \text{in the fluid region } j, \tag{1}$$

where subscript 1 refers to the fluid region 1 ($-\infty < x < 0$, $0 < y < H$) and 2 refers to the fluid region 2 ($0 < x < +\infty$, $0 < y < H$). The linearized free surface boundary condition is

$$\frac{\partial\phi_j}{\partial y} + K\phi_j = 0 \quad (j = 1, 2) \text{ on } y = 0, \tag{2}$$

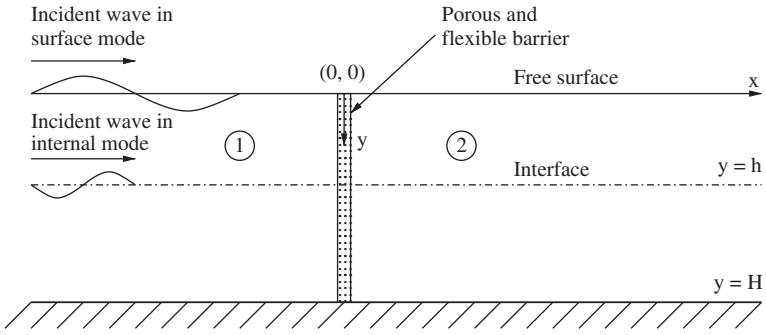

Fig. 1. Definition sketch.

where $K = \omega^2/g$, and g is the gravitational constant. The boundary condition at the interface requires that

$$\frac{\partial \phi_j}{\partial y} \quad \text{is continuous across } y = h \quad \text{and} \tag{3}$$

$$\left(\frac{\partial \phi_j}{\partial y} + K\phi_j\right)_{y=h^+} = s\left(\frac{\partial \phi_j}{\partial y} + K\phi_j\right)_{y=h^-} \quad (j = 1, 2) \text{ for } 0 < h < H, -\infty < x < \infty, \tag{4}$$

where s is the ratio of the densities of the upper fluid and the lower fluid, i.e. $s = \rho_1/\rho_2$ and has range $0 < s < 1.0$. The condition on the rigid bottom is given by

$$\frac{\partial \phi_j}{\partial y} = 0 \quad (j = 1, 2) \text{ on } y = H. \tag{5}$$

The radiation conditions are given by

$$\phi_1 \to \sum_{n=I}^{II} (I_n e^{ip_n x} + R_n e^{-ip_n x}) f_n(p_n, y) \quad \text{as } x \to -\infty, \tag{6}$$

and

$$\phi_2 \to \sum_{n=I}^{II} T_n e^{ip_n x} f_n(p_n, y) \quad \text{as } x \to \infty, \tag{7}$$

where I_I and I_{II} represent the incident wave amplitudes in SM (fast mode) and IM (slow mode), respectively, and are assumed to be very small in comparison with the undisturbed fluid depths h and $H - h$, respectively. R_I, T_I and R_{II}, T_{II} are the unknown reflected and transmitted wave amplitudes in SM and IM, respectively. It may be noted that p_I and p_{II} are wavenumbers for the incident waves in SM and IM, respectively. Similar definitions for the velocity potentials in a scattering problem for a two-layer fluid are given by Barthélemy et al. (2000).

The barrier is deflected horizontally with a displacement $\zeta(y, t) = \mathscr{R}e[\xi(y)\exp(-i\omega t)]$ and $\xi(y)$ denotes the complex deflection amplitude, which is assumed to be small compared to the water depth. The boundary condition on the porous barrier surface is given by

$$\frac{\partial \phi_j}{\partial x} = ik_0 G(\phi_2 - \phi_1) - i\omega\xi \quad (j = 1, 2) \text{ on } x = 0, 0 < y < H, \tag{8}$$

where $G = G_r + iG_i$ is the porous-effect parameter as defined by Yu and Chwang (1994) such that

$$G = \frac{\gamma(f + is^*)}{k_0 d(f^2 + s^{*2})} \tag{9}$$

in which γ is the porosity, f the resistance force coefficient, s^* the inertial force coefficient, d the thickness of the porous medium and k_0 the wavenumber of the incident wave (= either p_I or p_{II} depending on the mode of incident wave). In the present analysis two incident wave modes are considered at a time, hence without loss of generality, in all the present

calculations k_0 is taken as p_I. The real part G_r represents the resistance effect of the porous material against the seepage flow, while the imaginary part G_i denotes the inertia effect of the fluid inside the porous material.

It is assumed that the membrane is a thin, homogeneous and inextensible sheet with uniform mass m_s ($m_s = \rho_s d$, d is the thickness of the membrane, ρ_s is the uniform membrane mass density) under constant tension T. With these assumptions, the equation relating the displacement ξ from equilibrium to that of differential pressure P_s acting on the membrane at $x = 0$ can be obtained and is given as

$$\frac{\mathrm{d}^2\xi}{\mathrm{d}y^2} + \beta^2\xi = \begin{cases} \dfrac{\mathrm{i}\omega\rho_1}{T}(\phi_2 - \phi_1) & \text{for } 0<y<h, \\ \dfrac{\mathrm{i}\omega\rho_2}{T}(\phi_2 - \phi_1) & \text{for } h<y<H, \end{cases} \tag{10}$$

where $\beta = \omega\sqrt{m_s/T}$ is the barrier frequency parameter. The membrane is pinned at the free surface and the bottom, so the corresponding boundary conditions are

$$\xi(0) = 0, \quad \xi(H) = 0. \tag{11}$$

The continuity of deflection and slope of the membrane barrier across the interface yield

$$\xi(h^-) = \xi(h^+), \quad \xi'(h^-) = \xi'(h^+). \tag{12}$$

3. Method of solution

The spatial velocity potentials ϕ_j for $j = 1, 2$ satisfying Eq. (1) along with conditions (2)–(7) are expressed as

$$\phi_1 = \left(\sum_{n=I}^{II} I_n \mathrm{e}^{\mathrm{i}p_n x} + \sum_{n=I,II,1}^{\infty} R_n \mathrm{e}^{-\mathrm{i}p_n x}\right) f_n(p_n, y) \quad \text{for } x<0, \tag{13}$$

and

$$\phi_2 = \sum_{n=I,II,1}^{\infty} T_n \mathrm{e}^{\mathrm{i}p_n x} f_n(p_n, y) \quad \text{for } x>0, \tag{14}$$

where the eigenfunctions $f_n(p_n, y)$ are given by

$$f_n(p_n, y) = \begin{cases} \dfrac{\sinh p_n(H-h)\,[p_n \cosh p_n y - K \sinh p_n y]}{K\cosh p_n h - p_n \sinh p_n h} & \text{for } 0<y<h \\ \cosh p_n(H-y) & \text{for } h<y<H \end{cases} \quad (n = I, II, 1, 2, \ldots). \tag{15}$$

R_n and T_n for $n = I, II, 1, 2, 3, \ldots$ are unknown constants to be determined. The wavenumbers p_n ($n = I, II$ for positive real roots and $n = 1, 2, 3, \ldots$ for positive purely imaginary roots) are the roots of the dispersion relation in p as given by

$$(1-s)p^2 \tanh p(H-h) \tanh ph - pK[\tanh ph + \tanh p(H-h)] + K^2[s \tanh p(H-h) \tanh ph + 1] = 0. \tag{16}$$

The eigenfunctions $f_n(p_n, y)$ for $n = I, II, 1, 2, 3, \ldots$ are integrable in $0<y<H$ having a single discontinuity at $y = h$ and are orthogonal with respect to the inner product as defined by

$$\langle \phi, \psi \rangle = s\int_0^h \phi(y)\psi(y)\,\mathrm{d}y + \int_h^H \phi(y)\psi(y)\,\mathrm{d}y. \tag{17}$$

This may be easily seen from the fact that $f_n(p_n, y)$ for $n = I, II, 1, 2, 3, \ldots$ are the eigenfunctions associated with the self-adjoint operator

$$L\Theta \equiv \frac{\mathrm{d}^2\Theta}{\mathrm{d}y^2} = \lambda^2\Theta, \quad y \in (0, h) \cup (h, H),$$

corresponding to the eigenvalues $\lambda = p_n$ for $n = I, II, 1, 2, 3, \ldots$, and satisfying the fluid boundary conditions as given by

$$\Theta'(0) + K\Theta(0) = 0, \quad \Theta'(H) = 0.$$

The conditions at the point of discontinuity $y = h$ are given by

$$\Theta'(h-0) = \Theta'(h+0), \quad s[\Theta'(h-0) + K\Theta(h-0)] = [\Theta'(h+0) + K\Theta(h+0)],$$

where the prime denotes the first derivative with respect to y. Further, it may be noted that the orthogonality relation (17) reduces to the usual one in the single-layer fluid when $s = 1$.

Applying the continuity of ϕ_x (Eq. (8)) along the porous barrier on $x = 0$ and invoking the orthogonality relation (Eq. (17)) over $(0<y<h) \cup (h<y<H)$, we obtain

$$I_n - R_n = T_n \quad \text{for } n = I, II \quad \text{and} \quad R_n = -T_n \quad \text{for } n = 1, 2, 3, \ldots . \tag{18}$$

A general solution for the membrane governing equation (Eq. (10)) is of the form

$$\xi(y) = C' e^{i\beta y} + C'' e^{-i\beta y} - \frac{2i\omega\rho}{T} \sum_{n=I,II,1}^{\infty} \frac{R_n}{p_n^2 + \beta^2} f_n(p_n, y) \quad \text{for } 0<y<H, \tag{19}$$

where the arbitrary constants C', C'' and the fluid density ρ are defined as

$$C' = \begin{cases} C_1 & \text{for } 0<y<h, \\ C_3 & \text{for } h<y<H, \end{cases} \quad C'' = \begin{cases} C_2 & \text{for } 0<y<h, \\ C_4 & \text{for } h<y<H, \end{cases} \quad \rho = \begin{cases} \rho_1 & \text{for } 0<y<h, \\ \rho_2 & \text{for } h<y<H. \end{cases}$$

Substituting this general solution for ξ (Eq. (19)) in Eq. (8) and using the relations in Eqs. (13), (14) and (18) the following expression is derived:

$$h_0(y) + \sum_{n=I,II,1}^{\infty} R_n h_n(y) = 0, \quad 0<y<H, \tag{20}$$

where

$$h_0(y) = \begin{cases} ip_I I_I f_I(p_I, y) + ip_{II} I_{II} f_{II}(p_{II}, y) + i\omega C_1 e^{i\beta y} + i\omega C_2 e^{-i\beta y} & \text{for } 0<y<h, \\ ip_I I_I f_I(p_I, y) + ip_{II} I_{II} f_{II}(p_{II}, y) + i\omega C_3 e^{i\beta y} + i\omega C_4 e^{-i\beta y} & \text{for } h<y<H \end{cases}$$

and

$$h_n(y) = \begin{cases} \left[\dfrac{2\omega^2\rho_1}{(p_n^2+\beta^2)T} - ip_n - 2ip_I G\right] f_n(p_n, y) & \text{for } 0<y<h \\ \left[\dfrac{2\omega^2\rho_2}{(p_n^2+\beta^2)T} - ip_n - 2ip_I G\right] f_n(p_n, y) & \text{for } h<y<H \end{cases} \qquad (n = I, II, 1, 2, \ldots).$$

Let

$$Q(y) = h_0(y) + \sum_{n=I,II,1}^{N} R_n h_n(y) \text{ for } 0<y<H. \tag{21}$$

Applying the least-squares method,

$$\int_0^H \bar{Q}(y) \frac{\partial Q(y)}{\partial R_n} \, dy = 0 \quad \text{for } n = I, II, 1, 2, \ldots, N, \tag{22}$$

where the bar denotes the complex conjugate. This provides $N + 2$ linear equations with $N + 6$ unknowns, as $h_0(y)$ involves four extra unknowns C_1, C_2, C_3 and C_4. These $N + 2$ linear equations in the integral form are

$$\int_0^H \left[h_0(y) + \sum_{n=I,II,1}^{N} R_n h_n(y)\right] \bar{h}_i(y) \, dy = 0 \quad \text{for } i = I, II, 1, 2, \ldots, N. \tag{23}$$

The end conditions on the barrier as in Eq. (11) and the continuity conditions at the interface as in Eq. (12) yield another four linear equations as given by

$$C_1 + C_2 - \frac{2i\omega\rho_1}{T} \sum_{n=I,II,1}^{N} \frac{R_n}{p_n^2 + \beta^2} f_n(p_n, 0) = 0, \tag{24}$$

$$C_3 e^{i\beta H} + C_4 e^{-i\beta H} - \frac{2i\omega\rho_2}{T} \sum_{n=I,II,1}^{N} \frac{R_n}{p_n^2 + \beta^2} f_n(p_n, H) = 0, \tag{25}$$

$$C_1 e^{i\beta h} + C_2 e^{-i\beta h} - \frac{2i\omega\rho_1}{T} \sum_{n=I,II,1}^{N} \frac{R_n}{p_n^2 + \beta^2} f_n(p_n, h^-) = C_3 e^{i\beta h} + C_4 e^{-i\beta h} - \frac{2i\omega\rho_2}{T} \sum_{n=I,II,1}^{N} \frac{R_n}{p_n^2 + \beta^2} f_n(p_n, h^+) \tag{26}$$

and

$$i\beta C_1 e^{i\beta h} - i\beta C_2 e^{-i\beta h} - \frac{2i\omega\rho_1}{T} \sum_{n=I,II,1}^{N} \frac{R_n}{p_n^2 + \beta^2} f'_n(p_n, h^-) = i\beta C_3 e^{i\beta h} - i\beta C_4 e^{-i\beta h} - \frac{2i\omega\rho_2}{T} \sum_{n=I,II,1}^{N} \frac{R_n}{p_n^2 + \beta^2} f'_n(p_n, h^+), \tag{27}$$

with the prime denoting the derivative with respect to y. The system of Eqs. (23)–(27) is solved to compute and analyse various physical quantities of interest.

4. Numerical results and discussion

In the present section, numerical results on the combined effect of porosity and membrane tension are discussed, to analyse the performance of the membrane barrier in the two-layer fluid for various nondimensional parameters. For convenience, the wave and membrane parameters are given in terms of nondimensional values of wavenumber $p_I H$, water depth h/H, fluid density ratio s, porous-effect parameter G, membrane tension $T' = T/(\rho g h^2)$, and membrane mass $m' = m/\rho h$. The membrane mass m' is kept fixed ($m' = 0.1$) throughout the analysis as the effect of membrane mass on the performance characteristic of the barrier is insignificant (Kim and Kee, 1996; Lo, 1998). The reflection and

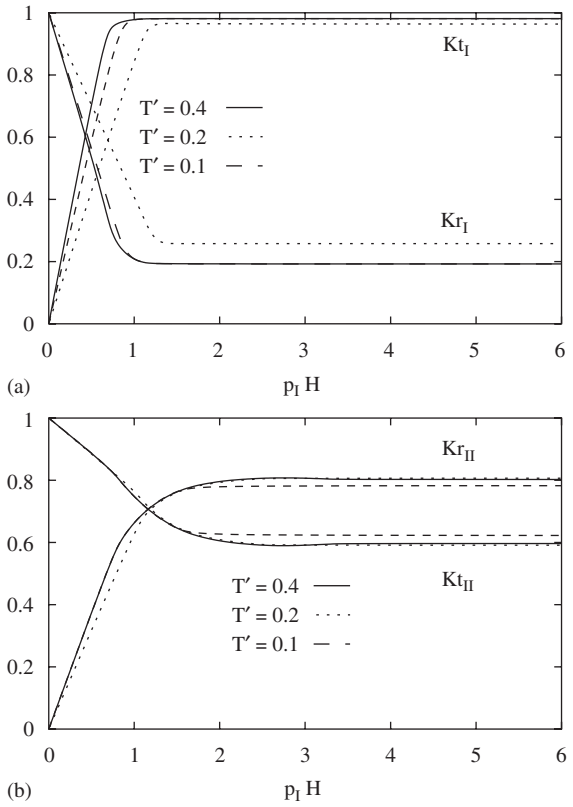

Fig. 2. Reflection and transmission coefficients in (a) SM and (b) IM versus $p_I H$ for different T' values at $G = 1 + 2i$, $s = 0.75$ and $h/H = 0.5$.

transmission coefficients are defined by

$$Kr_I = \left|\frac{R_I}{I_I}\right| \quad \text{and} \quad Kt_I = \left|\frac{T_I}{I_I}\right| \quad \text{in SM},$$
$$Kr_{II} = \left|\frac{R_{II}}{I_{II}}\right| \quad \text{and} \quad Kt_{II} = \left|\frac{T_{II}}{I_{II}}\right| \quad \text{in IM}. \tag{28}$$

The wave transmission across a permeable membrane barrier is governed by two combined phenomena. When a train of waves approaches a permeable flexible barrier, seepage flow induced by waves penetrates through the barrier and waves are reproduced with some dissipation after transmission. On the other hand, due to deformation of the membrane barrier, the waves are regenerated in the downstream side, even if there is no flow across the barrier.

4.1. Energy reflection and transmission

In general, the energy reflection and transmission provide one of the major criteria in deciding the effectiveness of the barrier. In this subsection, the effects of various nondimensional physical parameters on energy reflection and transmission in both SM and IM are analysed. For the sake of simplicity, all results in the present subsection are analysed with respect to the normalized SM wavenumber $p_I H$ by allowing the normalized IM wavenumber $p_{II} H$ to vary based on the two-layer fluid dispersion relation (Eq. (16)). It is observed from the general trend of wave reflection in SM that the wave reflection decreases from its peak to a certain value in the shallow water region and thereafter it attains a constant value. On the other hand, the wave reflection in IM increases from zero to a certain value in the shallow water region and thereafter it attains a constant value (see Figs. 2–5). Similar results are obtained for wave reflection by a flexible membrane barrier in a single-layer fluid by Lo (2000) and Lee and Lo (2002) [see Fig. 3(a) of Lo

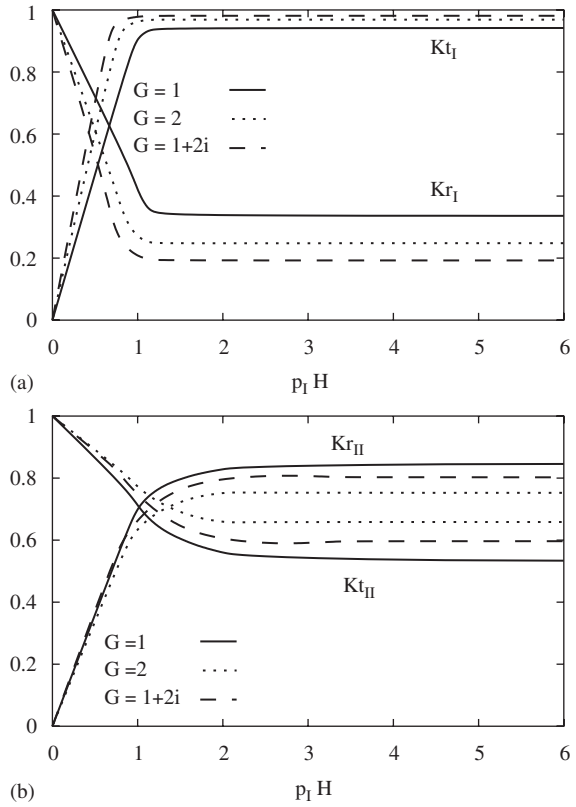

Fig. 3. Reflection and transmission coefficients in (a) SM and (b) IM versus $p_I H$ for different G values at $h/H = 0.5$, $s = 0.75$ and $T' = 0.4$.

(2000) and Fig. 5 of Lee and Lo (2002)]. Furthermore, the wave reflection in SM is found to be significantly smaller than the wave reflection in IM, which suggests that a membrane barrier is more effective in IM wave motion than in SM wave motion. Similar observations are reported by Manam and Sahoo (2005).

In Fig. 2(a,b), the reflection and transmission coefficients in SM and IM, respectively, are plotted against $p_I H$, for different values of membrane tension parameter T'. It is observed that higher wave transmission and lower wave reflection occur in SM whereas lower wave transmission and higher wave reflection occur in IM over the range of practical interest.

The variation of reflection and transmission coefficients versus $p_I H$ for both SM and IM are plotted in Fig. 3(a,b), respectively, for different values of the porous-effect parameter G. In general, the wave reflection in both SM and IM increases with a decrease in the value of $|G|$ and a reverse trend is observed in the case of wave transmission. This is expected, because an increase in porosity not only allows more waves to pass through the barrier but also reduces the membrane barrier resistance to the wave motion.

The effects of nondimensional water depth h/H of two fluids on the reflection and transmission coefficients in SM and IM are shown in Fig. 4(a,b), respectively. In SM wave motion it is observed that the wave transmission is lower and the wave reflection is higher for a thinner upper layer, i.e. for $h/H = 0.25$ (Fig. 4(a)). However, except for very small values of $p_I H$ the wave reflection and transmission are same for $h/H = 0.5$ and 0.75. On the other hand, an opposite trend is observed in the case of IM wave motion where the wave transmission is higher and the wave reflection is lower for a thinner upper layer, i.e. $h/H = 0.25$ (Fig. 4(b)), almost over the entire range of interest. This is because of the resonating interaction of surface and internal waves when the free surface is close to the interface.

The reflection and transmission coefficients versus $p_I H$ are plotted in SM and IM for different fluid density ratios s in Fig. 5(a,b), respectively. In Fig. 5(a) it is observed that the fluid density ratio s has negligible effect on both wave reflection and transmission for SM wave motion. However, the wave reflection in SM is observed to be marginally

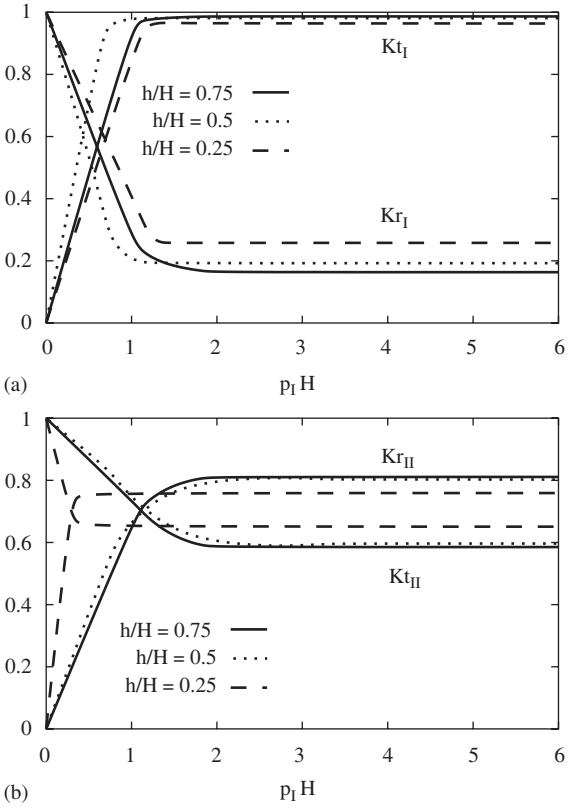

Fig. 4. Reflection and transmission coefficients in (a) SM and (b) IM versus $p_I H$ for different h/H ratios at $G = 1 + 2i$, $s = 0.75$ and $T' = 0.4$.

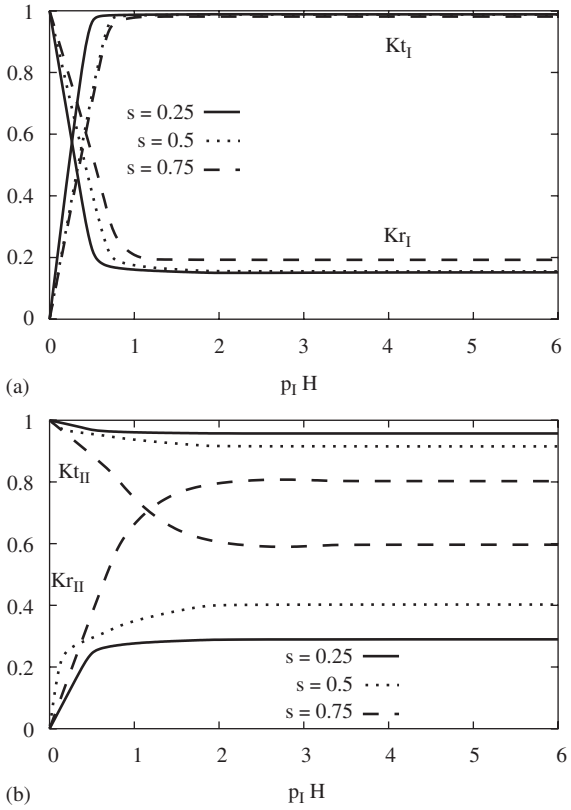

Fig. 5. Reflection and transmission coefficients in (a) SM and (b) IM versus $p_I H$ for different s values at $h/H = 0.5$, $G = 1 + 2\mathrm{i}$ and $T' = 0.4$.

higher for a large value of s ($s = 0.75$). On the other hand, the wave reflection increases and the wave transmission decreases for IM wave motion with an increase in fluid density ratio (Fig. 5(b)). This nature of the wave transmission in IM may be due to the high interface elevation as the fluid density ratio s approaches unity (Kundu and Cohen, 2002; Milne-Thomson, 1996).

4.2. Free surface and interface elevations

In this subsection, the nature of free surface elevation η_{fs} and interface elevation η_{int} versus nondimensional distance x/λ_I are plotted after normalizing with respect to the amplitude of the incident waves in the SM. This normalization gives a clear understanding about the amplitude of the free surface elevation to that of interfacial wave elevation. The free surface and interface elevations near the barrier are the result of mutual interaction of propagating and evanescent modes of both surface and internal waves (see Figs. 6–8). Hence the free surface and interface elevations in a two-layer fluid are combinations of two prominent wave patterns which are referred to as primary and secondary wave patterns in the present paper. The primary pattern is the one which is generated due to SM wave motion and the secondary wave pattern is that developed due to the IM wave motion. In general, it is observed that the interface elevation is much larger than that of the free surface elevation when either the densities of the two fluids are very close or in the case when the interface and free surface are close to each other. A similar situation exists in a real ocean, as explained theoretically in Milne-Thomson (1996, p. 445). One of the reasons for such a high wave amplitude may be due to the resonating interaction between the waves in SM and IM.

Fig. 6(a,b) shows the pattern of the free surface and interface elevations, respectively, for different values of membrane tension parameter T'. The effect of change in tension T' is significant only near the locations of local maxima and minima of the secondary wave pattern in the case of free surface elevation, Fig. 6(a). On the other hand, the interface elevation is found to be independent of the variation in membrane tension (see Fig. 6(b)).

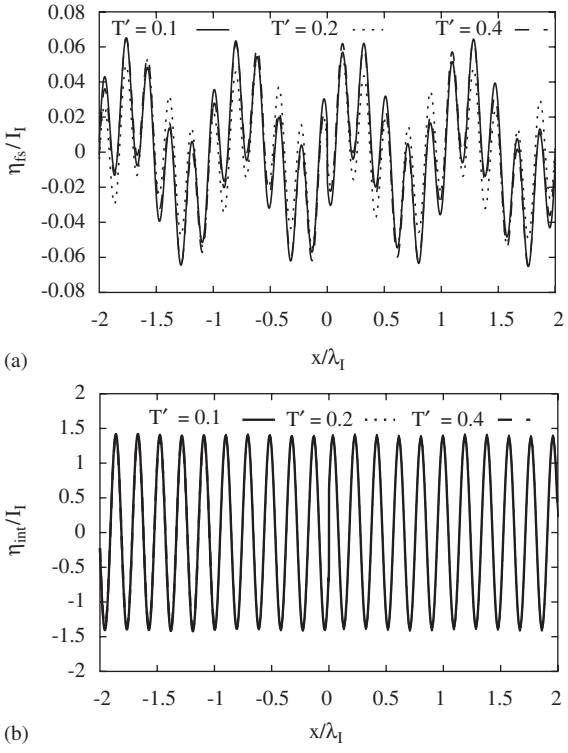

Fig. 6. (a) Free surface and (b) interface elevation versus x/λ_I for different T' values at $p_I H = 1.0$, $h/H = 0.5$, $G = 1 + 2i$ and $s = 0.75$.

Variations of free surface and interface elevations at different h/H ratios are shown in Fig. 7(a,b), respectively. It is observed that as the interface and free surface come nearer, the amplitudes of both free surface and interface elevations become higher. This may be due to the resonating interaction between the waves in SM and IM. The magnitude of the primary and secondary wave pattern amplitudes of the free surface elevation are of same order for small h/H ratio (Fig. 7(a)). This is due to the fact that the interface elevation increases rapidly when free surface and interface are close to each other (see Fig. 7 (b)).

Fig. 8(a,b) shows the pattern of the free surface and interface elevations for different fluid density ratios s. It is observed that the amplitude of the free surface elevation increases with decrease in the fluid density ratio s (Fig. 8(a)). On the other hand, an opposite trend is observed in case of interface elevation where it increases with an increase in fluid density ratio. As the fluid density ratio s approaches one, the secondary wave pattern of the free surface and the interface elevations amplify rapidly, which is a well-known phenomenon in the case of interfacial waves [see Kundu and Cohen (2002) and Milne-Thomson (1996)]. It is important to note that among the elevations, the interface depends heavily on the density ratio s. The reason for this is that the amplitudes of waves in IM are very sensitive to the change in density ratio s, whereas the waves in SM are least affected by the change in the value of s. Hence interface elevations change sharply with the change in parameter s, whereas free surface elevations are comparatively less affected by the change in the value of s. The variation in free surface elevations with the change in s is mainly due to the existence of the secondary wave pattern, which is again caused by the internal waves. This is the reason why, in Fig. 5, the reflection and transmission coefficients in IM are more dependent on s than those in SM. Interestingly, when $s = 0.25$, the free surface elevation is free from secondary waves, as in this case the internal waves have very small amplitude. Furthermore, it is observed that with increase in the value of s the wavelength of interfacial waves reduces and very short waves are observed as s approaches unity.

The local effects are not visible in the elevation plots because the magnitude of the contribution of local effects is insignificant as compared to that of propagating modes in SM and IM in the present study. Moreover, their contribution decays quickly as one moves away from the barrier (either left or right) because of the exponential decay of the multiplication factor in the velocity potential. There is always a discontinuity in elevation as the waves pass the

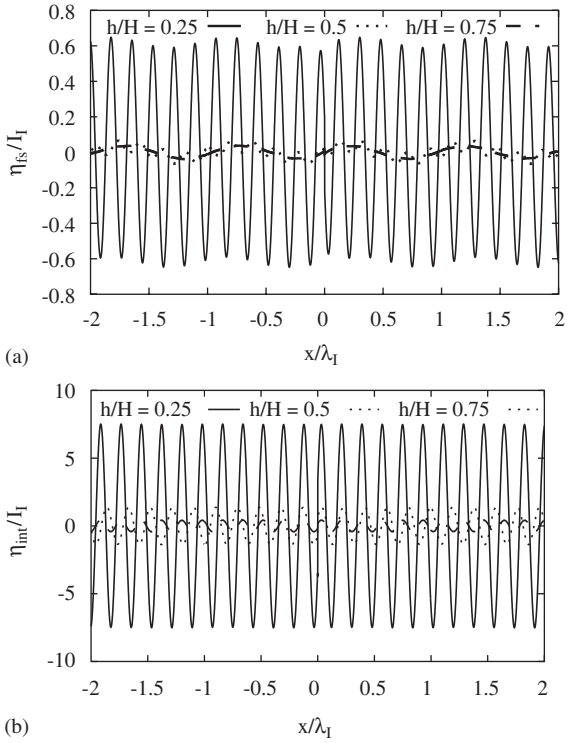

Fig. 7. (a) Free surface and (b) interface elevation versus x/λ_I for different h/H ratios at $p_I H = 1.0$, $G = 1 + 2i$, $s = 0.75$ and $T' = 0.4$.

barrier. However, in the present case the magnitude of the discontinuity is very small because the porous membrane offers very little resistance to waves. The discontinuity is only apparent in Fig. 8(a) for $s = 0.25$.

4.3. Response of the membrane barrier

In the present subsection, the variation of membrane barrier response ξ normalized with respect to incident wave amplitude I_I in SM is analysed for various membrane and two-layer fluid parameters. In all of Figs. 9–12, the vanishing nature of membrane response at the two ends is because the membrane is fixed at those points.

Variation of normalized membrane response $|\xi/I_I|$ for different h/H ratios is plotted versus normalized vertical position y/H in Fig. 9. It is observed that the barrier has higher deflection amplitude at a location nearer to the interface. This is due to the propagation of surface and interfacial waves at the interface in a two-layer fluid. However, the deflection is found to be higher for small h/H ratio (the interface is closer to the free surface). This is because of the higher free surface and interface elevation as observed in Fig. 7.

Variation of the normalized membrane response $|\xi/I_I|$ is plotted versus normalized vertical position y/H for different values of fluid density ratio s in Fig. 10. The membrane deflection is found to increase with the increase in fluid density ratio s. The reasons for these observations are clear from the nature of free surface and interface elevations in Fig. 8(a,b). However, nearer to the free surface, the membrane deflection in the upper fluid domain is found to be high for low fluid density ratio $s = 0.25$, as in this case the amplitude of free surface elevation is found to be quite high (see Fig. 8(a)).

The normalized membrane response $|\xi/I_I|$ for various values of membrane tension parameter T' is plotted versus normalized vertical position y/H in Fig. 11. It is clear from Fig. 11 that the membrane deflection increases with decrease in membrane tension. This is expected, because a reduction in membrane tension leads to a reduction in the stiffness of the membrane against the wave motion and leads to a higher membrane deflection.

In Fig. 12 the normalized membrane response $|\xi/I_I|$ is plotted versus normalized vertical position y/H for different values of the porous-effect parameter G. A high membrane deflection is observed for higher values of the imaginary part of the porous-effect parameter G (the inertia effect of the fluid inside the porous barrier).

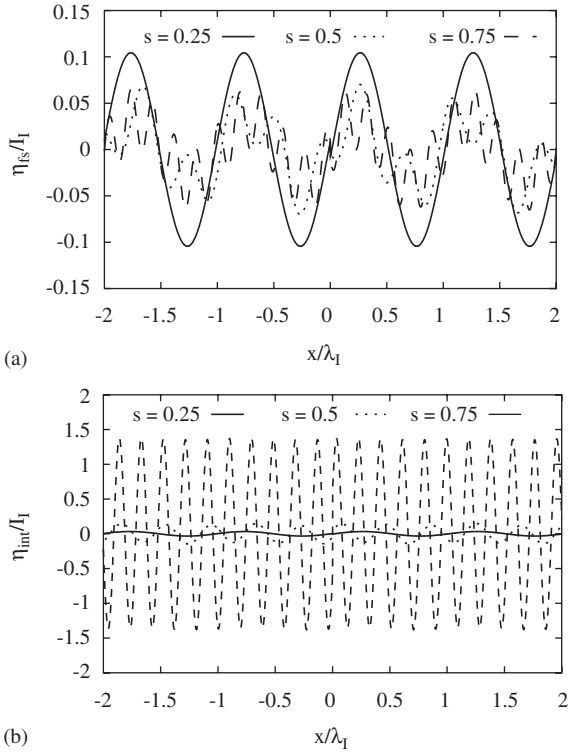

Fig. 8. (a) Free surface and (b) interface elevation versus x/λ_I for different s values at $p_I H = 1.0$, $h/H = 0.5$, $G = 1 + 2i$ and $T' = 0.4$.

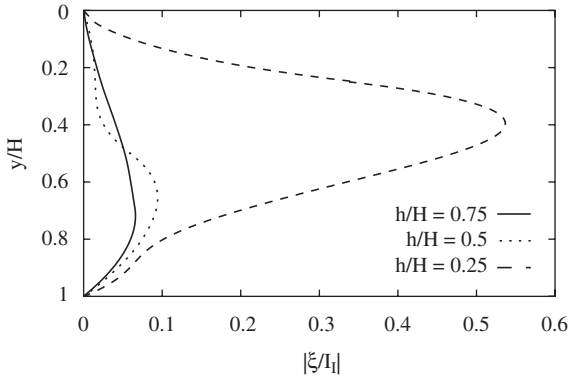

Fig. 9. Membrane displacement versus y/H for different h/H ratios at $s = 0.75$, $p_I H = 1.0$, $T' = 0.4$ and $G = 1 + 2i$.

5. Concluding remarks

The performance of a wave barrier comprising of a vertical flexible porous membrane, tensioned and pinned both at the free surface and the seabed, is investigated in a two-layer fluid of finite depth, with the upper fluid having a free surface. The introduction of the new orthogonality relation (Eq. (17) has simplified the mathematical analysis for the problem in the two-layer fluid. In the case of a two-layer fluid, the interfacial wave elevation is found to be much higher than the wave propagating at the free surface in certain situations. Furthermore, it is observed that the wave reflection

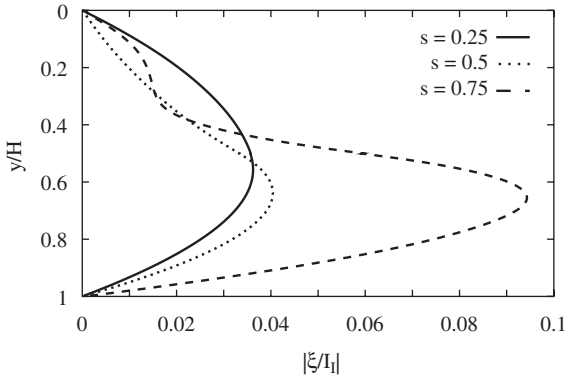

Fig. 10. Membrane displacement versus y/H for different s values at $h/H = 0.5$, $p_I H = 1.0$, $T' = 0.4$ and $G = 1 + 2\mathrm{i}$.

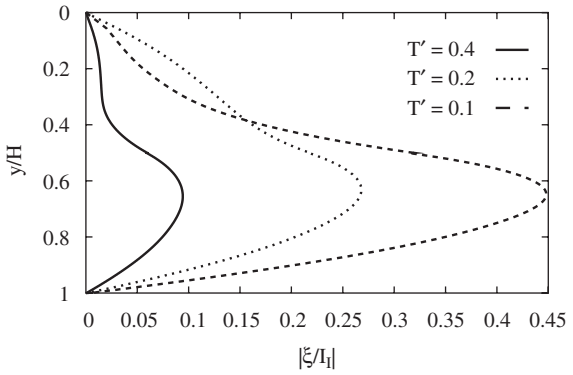

Fig. 11. Membrane displacement versus y/H for different T' values at $h/H = 0.5$, $s = 0.75$, $p_I H = 1.0$ and $G = 1 + 2\mathrm{i}$.

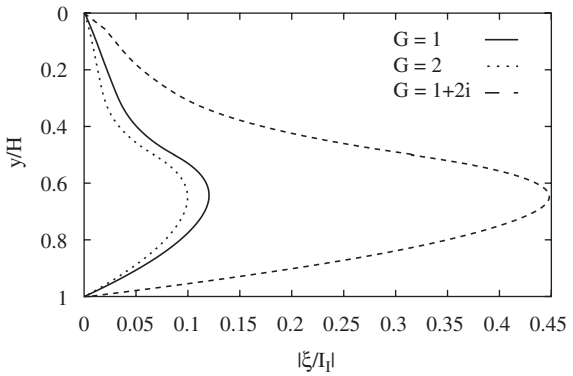

Fig. 12. Membrane displacement versus y/H for different G values at $s = 0.75$, $p_I H = 1.0$, $h/H = 0.5$ and $T' = 0.4$.

and transmission characteristics, free surface and interface elevations and barrier response are strongly dependent on the fluid density ratio and the interface location, as well as on barrier parameters like membrane tension and porosity. These observations are of considerable importance in the design of breakwaters either in locations where there exists a layer of fresh water above the salt water or in estuaries where fluid stratification plays a crucial role. A similar approach can be utilized to study more general problems in a two-layer fluid having a free surface.

Acknowledgements

P. Suresh Kumar acknowledges Indian Institute of Technology, Kharagpur for support as a research student. S.R. Manam acknowledges the financial support received from National Board for Higher Mathematics (NBHM) as a postdoctoral fellow. This research work is partially supported by Naval Research Board, New Delhi. The authors acknowledge the suggestions and comments of the reviewers and the editor to bring the paper to the present form.

References

Barthélemy, E., Kabbaj, A., Germain, J.P., 2000. Long surface waves scattered by a step in a two-layer fluid. Journal of Fluid Dynamics Research 26, 235–255.

Cadby, J.R., Linton, C.M., 2000. Three-dimensional water-wave scattering in two-layer fluids. Journal of Fluid Mechanics 423, 155–173.

Cho, I.H., Kee, S.T., Kim, M.H., 1998. Performance of dual flexible membrane wave barriers in oblique waves. ASCE Journal of Waterway, Port, Coastal, and Ocean Engineering 124, 21–30.

Chwang, A.T., 1983. A porous-wavemaker theory. Journal of Fluid Mechanics 132, 395–406.

Chwang, A.T., Chan, A.T., 1998. Interaction between porous media and wave motion. Annual Review of Fluid Mechanics 30, 53–84.

Kee, S.T., Kim, M.H., 1997. Flexible membrane wave barrier. II: floating/submerged buoy-membrane system. ASCE Journal of Waterway, Port, Coastal, and Ocean Engineering 123, 82–90.

Kim, M.H., Kee, S.T., 1996. Flexible-membrane wave barrier. I: analytic and numerical solutions. ASCE Journal of Waterway, Port, Coastal, and Ocean Engineering 122, 46–53.

Kundu, P.K., Cohen, I.M., 2002. Fluid Mechanics, second ed. Academic Press, San Diego, CA, USA.

Lamb, H., 1932. Hydrodynamics, sixth ed. Cambridge University Press, Cambridge (reprinted 1993).

Leach, P.A., McDougal, W.G., Sollitt, C.K., 1985. Hinged floating breakwater. ASCE Journal of Waterway, Port, Coastal, and Ocean Engineering 111, 895–909.

Lee, J.F., Chen, C.J., 1990. Wave interaction with hinged flexible breakwater. Journal of Hydrodynamic Research 28, 283–295.

Lee, M.M., Chwang, A.T., 2000. Scattering and radiation of water waves by permeable barriers. Physics of Fluids 12, 54–65.

Lee, W.K., Lo, E.Y.M., 2002. Surface-penetrating flexible membrane wave barrier of finite draft. Ocean Engineering 29, 1781–1804.

Linton, C.M., McIver, M., 1995. The interaction of waves with horizontal cylinders in two-layer fluids. Journal of Fluid Mechanics 304, 213–229.

Lo, E.Y.M., 1998. Flexible dual membrane wave barrier. ASCE Journal of Waterway, Port, Coastal, and Ocean Engineering 124, 264–271.

Lo, E.Y.M., 2000. Performance of a flexible membrane wave barrier of a finite vertical extent. Journal of Coastal Engineering 42, 237–251.

Manam, S.R., Sahoo, T., 2005. Waves past porous structures in a two-layer fluid. Journal of Engineering Mathematics 52, 355–377.

Milne-Thomson, L.M., 1996. Theoretical Hydrodynamics. Dover, New York.

Sherief, H.H., Faltas, M.S., Sadd, E.I., 2003. Forced gravity waves in two-layered fluids with the upper fluid having a free surface. Canadian Journal of Physics 81, 675–689.

Sollitt, C.K., Lee, C.P., McDougal, W.G., 1986. Mechanically coupled flap type breakwaters: theory and experiments. In: Proceedings of the 20th ASCE Coastal Engineering Conference, New York, pp. 2445–2462.

Stokes, G.G., 1847. On the theory of oscillatory waves. Transactions of the Cambridge Philosophical Society 8, 441–455.

Wang, K.H., Ren, X., 1993. Water waves on flexible and porous breakwaters. ASCE Journal of Engineering Mechanics 119, 1025–1047.

Wehausen, J.V., Laitone, E.V., 1960. In: Flügge, S. (Ed.), Handbuch der Physik, vol. 9. Springer, Berlin, pp. 446–778.

Williams, A.N., 1993. Dual floating breakwater. Ocean Engineering 20, 215–232.

Williams, A.N., Geiger, P.T., McDougal, W.G., 1991. Flexible floating breakwater. ASCE Journal of Waterway, Port, Coastal, and Ocean Engineering 117, 429–450.

Yeung, R.W., Nguyen, T., 1999. Radiation and diffraction of waves in a two-layer fluid. In: Proceedings of the 22nd ONR Symposium on Naval Hydrodynamics, pp. 875–891.

Yu, X., Chwang, A.T., 1994. Wave induced oscillation in harbor with porous breakwaters. ASCE Journal of Waterway, Port, Coastal, and Ocean Engineering 120, 125–144.

Zilman, G., Miloh, T., 1995. Hydrodynamics of a body moving over a mud layer—Part I: wave resistance. Journal of Ship Research 38, 194–201.

Zilman, G., Kagan, L., Miloh, T., 1996. Hydrodynamics of a body moving over a mud layer—Part II: added-mass and damping coefficients. Journal of Ship Research 40, 39–45.